IMA Journal of Mathematics Applied in Medicine and Biology (1999) **16**, 369–393

Modelling corneal epithelial wound closure in the presence of physiological electric fields via a moving boundary formalism

E. A. GAFFNEY[†]
The School of Mathematics and Statistics, The University of Birmingham, Edgbaston Birmingham B15 2TT, UK

P. K. MAINI
Centre for Mathematical Biology, Mathematical Institute, 24–29 St Giles', Oxford OX1 3LB, UK

C. D. MCCAIG AND M. ZHAO
Department of Biomedical Sciences, University of Aberdeen, UK

J. V. FORRESTER
Department of Ophthalmology, University of Aberdeen, UK

[Received 17 June 1998 and in revised form 9 April 1999]

A new framework for the modelling of corneal epithelial wound healing is presented, which can include the presence of a physiological electric field. The difficulty inherent in the inclusion of this biological phenomenon motivates our use of a moving boundary formalism. A key conclusion is that the model predicts a linear relation between the wound healing speed and the physiological electric field strengths over a physiologically large range of electric field strength. Another key point is that this linear relationship between electric field strength and wound healing speed is robust to variations in critical parameters that are difficult to estimate. The linearity is also robust to different realizations of the modelling framework presented.

Keywords: moving boundaries; corneal epithelial wound healing.

1. Introduction

Quantitative data is increasingly becoming available from experimental investigations of corneal epithelial wound healing. There is also the promise of remarkably detailed observational insight into cell kinetics and cell dynamics, and perhaps large amounts of multidimensional quantitative data too, due to the very recent development of confocal microscopy techniques for the *in-vivo* corneal epithelium (Beebe & Masters, 1996; Masters, 1995; Tsai *et al.*, 1997). Consequently, mathematical and computational modelling, though currently in its infancy in this particular area, may reasonably be expected to play an ever increasing role in the coordination and development of a quantitative understanding of the corneal epithelium and its complex wound healing response.

[†]Author for correspondence (Email: eag@for.mat.bham.ac.uk).

In this paper the modelling of the corneal epithelium and its repair is considered within a simplified picture, as outlined by Gaffney *et al.* (1997). Pathological possibilities such as angiogenesis and conjunctival invasion of the cornea are discounted, as are innervation, the immunological system, and many other intrinsic biological features. One thus initially considers a system of epithelial cells in various states of differentiation on a basal lamina. The tissue dynamics are controlled by numerous types of cell–cell and cell–substrate interactions. These interactions, together with the cell proliferation and differentiation rates and extracellular matrix component synthesis rates, are critically dependent on dozens of different growth factors. These growth factors, often referred to as cytokines, originate from numerous possible sources including cell secretions, tear fluid, and in a wounded cornea, cell debris, and possibly exogenous application.

Even the above simplified picture is too complex to be modelled. Focusing on specifics within this picture has nonetheless been fruitful. A recent model, developed by Dale *et al.* (1994a,b), considers a single generic cell type and a single generic stimulus. Considering how such entities would interact results in a phenomenological model of two coupled nonlinear partial differential equations. Such a model, and the travelling wave equations derived from it, predicted wave speeds that agreed with experimental observations for biologically reasonable parameters.

Recent experimental investigations have revealed that cell migration near the edge of a corneal epithelial wound occurs in the presence of a small, physiological, electric field. Further studies have shown that even these small electric fields are capable of influencing the migration of corneal epithelial cells, and moreover describe the manner of this influence (Zhao *et al.*, 1996a,b,1997). The aim of this paper is thus to construct a reasonably simple modelling framework capable of predicting the variation of a measure of the corneal epithelium regenerative ability, namely the wound healing speed, including effects arising from electric fields. This is particularly important as a common hypothesis is that electric fields of physiological strength could be utilized for the regulation and control of a variety of wound healing responses (Borgens *et al.*, 1989; McCaig & Zhao, 1997).

More generally, moving boundary modelling techniques have found successful application in many other areas of mathematical modelling. They have not, however, been widely applied to biomathematical studies. This is despite the possible relevance of this technique in modelling invasive biological phenomena, such as wound healing and cancer metastasis, as well as in the field of ecology. Thus, at a more general level, it is hoped that this paper illustrates the possible use of moving boundaries within biomathematics and encourages the consideration of such techniques within this field.

In Section 2, we summarize the relevant corneal epithelial electrophysiology, which motivates our choice of modelling framework. In Section 3, we proceed to formulate the modelling framework, and discuss model nondimensionalization and parameter estimation. Modelling results and predictions are presented in Section 4, with an emphasis on the relation between the electric field strength and the model prediction of the wound healing speed. This is followed by an illustration of model robustness in Section 5 and by conclusions in Section 6.

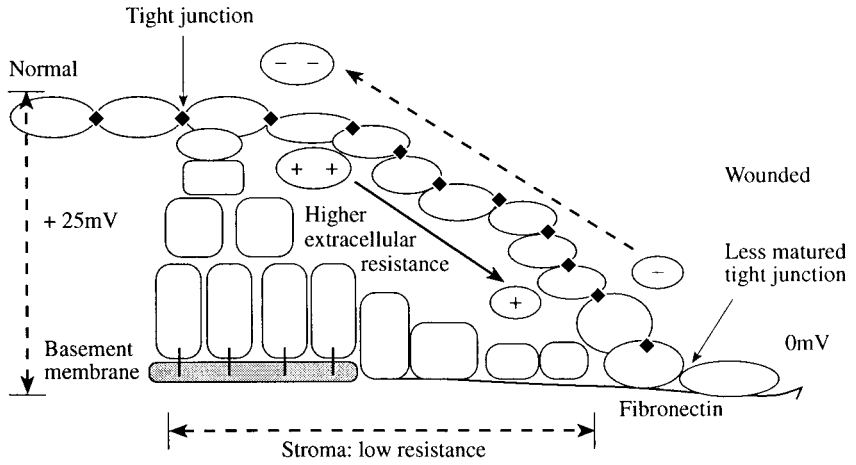

FIG. 1. A schematic illustrating the potential role of lateral electric fields in directing corneal epithelial migration at a wound edge. The cells are represented by the outlines of rectangles and ellipses, where the shapes of these symbols crudely correspond to the shape of the actual cells.

2. Experimental motivation for modelling

2.1 *Electrophysiological phenomena*

It has recently been noted that direct current (d.c.) electric fields of physiological strength can influence the *in-vitro* migration of bovine and human corneal epithelial cells (Zhao *et al.*, 1996a,b). Indeed, d.c. electric fields have been measured directly at the wound margin in experimentally lesioned bovine corneal epithelium (Chiang *et al.*, 1992).

The electric field arises because the transcorneal potential difference at the site of the wound is short-circuited and collapses, but a normal potential difference is maintained by the epithelium at distances more than 1 mm from the wound margin; see Fig. 1. Migrating corneal epithelial cells at a wound front, therefore, of necessity, are moving in the presence of a laterally oriented d.c. electric field.

In Fig. 1, the transcorneal potential difference (PD) indicated on the left (by the +25 mV label) is supported by the high resistance of the tight junctions in the upper sheet of epithelial cells. At the wound the PD collapses to zero. Direct measurements indicate that the lateral fields in the tear fluid are higher than those in the stroma. The lateral fields, and their relative electric potentials, are indicated by the minus and double minus signs; the arrow between these minus signs points in the direction of increasingly negative electric potential. At subepithelial stromal levels the resistance to current flow is low, and thus only very small electric fields can be established. However, the relevant subepithelial voltage drop immediately below the top sheet of corneal epithelium has not been measured and is likely to be substantial, given the tight packing of these differentiated and flattened cells. (In corneal epithelial wounds, the tight junction specific protein, occludin is present just one cell back from the leading edge (Danjo & Gipson, 1998).) The electric potential below the top sheet could consistently be given as indicated by the double plus and plus signs, again

connected by an arrow pointing in the direction of increasingly negative electric potential (Zhao *et al.*, 1999a). The lower surface of the cells of a sliding sheet therefore would be migrating towards a cathode, as indicated by the potential difference apparent across such cells depicted by the plus and minus sign above. See (Zhao *et al.*, 1999a) for more details. In our model, we do not consider the above vertical heterogeneity of the electric field, thus enabling a one-dimensional model, as discussed further in Section 3.2. It is clear, however, that a useful extension of the modelling will be to generalize to include possible effects from vertical heterogeneity of the electric field (see Section 6).

When cultured in a d.c. electric field, the random walk displayed by such cells in the absence of external stimuli is superimposed with a drift directionality towards the electric field cathode. The *magnitude* of the velocity of the cellular movement appears unchanged (Zhao *et al.*, 1996a). The effect is magnified when groups of cells are clustered, as has been demonstrated experimentally (Zhao *et al.*, 1996b), as well as being previously hypothesized theoretically (Cooper, 1984). Moreover, the cathodally directed migration of bovine corneal epithelial cells is enhanced when cells are cultured on fibronectin, which is secreted as an early response to wounding and which forms a provisional extracellular matrix for corneal epithelial cell migration (Zhao *et al.*, 1999a).

2.2 *Motivation for a moving boundary model*

The above biological scenario poses a specific problem for modelling, as we now describe. Typically, when developing a framework for modelling investigations of wound healing processes one presupposes that all stimuli are *a priori* known functions of the dependent and independent variables. However, for the case of the electric field described in the previous section this is not the case. As noted above, only cells within a relatively small distance, or *skin depth*, of less than 1 mm from the migrating wound edge are affected by the electric field. This means the stimulus resulting from the electric field critically depends on the position of the wound edge, which is not known *a priori*. This key difficulty means that standard biomathematical modelling via the use of reaction diffusion equations on a fixed domain is inappropriate.

In this paper, we attempt to overcome such problems by introducing a moving boundary, understood in the mathematical sense, at the migrating edge of the wound. By this, we mean that one imposes the presence of some discontinuity in the corneal epithelial cell density, whose movement is uniquely determined once jump conditions in the cell density and its first derivative are assigned at the discontinuity. The jump conditions that are used in the modelling are obtained from biological considerations. An overview of the modelling framework is presented below, and we proceed to consider two realizations of the modelling framework.

We note that one might, for example, be tempted to model the electric field via a cell density dependence, as generally it would be expected that the cell density decreases on approaching the wound edge. However, previous studies (e.g. see Fig. 4 of Dale *et al.*, 1994b; Figs 1.4–1.9 of Dale, 1995; Gaffney *et al.*, 1997) show that the cell density in traditional reaction diffusion models of corneal epithelial wound healing is nonmonotonic in the vicinity of the wound edge at early times, and the details of this behaviour is highly parameter dependent and varies with time. This strongly suggests that to integrate the model incorporating the electric field via considering a cell density dependent convection

connected by an arrow pointing in the direction of increasingly negative electric potential (Zhao *et al.*, 1999a). The lower surface of the cells of a sliding sheet therefore would be migrating towards a cathode, as indicated by the potential difference apparent across such cells depicted by the plus and minus sign above. See (Zhao *et al.*, 1999a) for more details. In our model, we do not consider the above vertical heterogeneity of the electric field, thus enabling a one-dimensional model, as discussed further in Section 3.2. It is clear, however, that a useful extension of the modelling will be to generalize to include possible effects from vertical heterogeneity of the electric field (see Section 6).

When cultured in a d.c. electric field, the random walk displayed by such cells in the absence of external stimuli is superimposed with a drift directionality towards the electric field cathode. The *magnitude* of the velocity of the cellular movement appears unchanged (Zhao *et al.*, 1996a). The effect is magnified when groups of cells are clustered, as has been demonstrated experimentally (Zhao *et al.*, 1996b), as well as being previously hypothesized theoretically (Cooper, 1984). Moreover, the cathodally directed migration of bovine corneal epithelial cells is enhanced when cells are cultured on fibronectin, which is secreted as an early response to wounding and which forms a provisional extracellular matrix for corneal epithelial cell migration (Zhao *et al.*, 1999a).

2.2 *Motivation for a moving boundary model*

The above biological scenario poses a specific problem for modelling, as we now describe. Typically, when developing a framework for modelling investigations of wound healing processes one presupposes that all stimuli are *a priori* known functions of the dependent and independent variables. However, for the case of the electric field described in the previous section this is not the case. As noted above, only cells within a relatively small distance, or *skin depth*, of less than 1 mm from the migrating wound edge are affected by the electric field. This means the stimulus resulting from the electric field critically depends on the position of the wound edge, which is not known *a priori*. This key difficulty means that standard biomathematical modelling via the use of reaction diffusion equations on a fixed domain is inappropriate.

In this paper, we attempt to overcome such problems by introducing a moving boundary, understood in the mathematical sense, at the migrating edge of the wound. By this, we mean that one imposes the presence of some discontinuity in the corneal epithelial cell density, whose movement is uniquely determined once jump conditions in the cell density and its first derivative are assigned at the discontinuity. The jump conditions that are used in the modelling are obtained from biological considerations. An overview of the modelling framework is presented below, and we proceed to consider two realizations of the modelling framework.

We note that one might, for example, be tempted to model the electric field via a cell density dependence, as generally it would be expected that the cell density decreases on approaching the wound edge. However, previous studies (e.g. see Fig. 4 of Dale *et al.*, 1994b; Figs 1.4–1.9 of Dale, 1995; Gaffney *et al.*, 1997) show that the cell density in traditional reaction diffusion models of corneal epithelial wound healing is nonmonotonic in the vicinity of the wound edge at early times, and the details of this behaviour is highly parameter dependent and varies with time. This strongly suggests that to integrate the model incorporating the electric field via considering a cell density dependent convection

term through the early time, initial transient, phase would be very difficult. One would have to know the cell density dependence, and this would be (i) highly sensitive to the parameter values, (ii) highly time dependent, and (iii) multiple valued, and thus the cell density dependence would be highly nontrivial. Thus clearly such an approach is inappropriate in general. (Though undoubtedly such an approach could be of use in understanding the properties of the large-time asymptotes of the solutions when the cell density is monotonic near the wound edge.)

3. The modelling framework

3.1 *Model geometry*

In the modelling below, we apply a moving boundary formalism to the simplest possible case, using a Cartesian coordinate system. This simplification is motivated by previous modelling experience; this indicates that use of axisymmetric cylindrical or axisymmetric spherical polars, which would be motivated by the geometry of the cornea, is not an important factor in modelling corneal epithelial wound healing (CEWH). This applies both for wound healing speeds (Dale *et al.*, 1994b; Gaffney *et al.*, 1997) and cell kinetics (Gaffney *et al.*, 1999).

3.2 *The generic features of the modelling framework*

The constituents of the model are:

- a generic corneal epithelial cell type,
- and a single chemical stimulus representing the net effects of growth factors and other possible stimuli.

The model must incorporate a migration mechanism for these constituents, which we detail below, especially for the novel aspects of the cellular migration. The chemical stimulus is assumed to spread rapidly across the cornea via tear film diffusion. In order to caricature transport mechanisms of chemical stimulus due to tear fluid convection and mixing arising from blinking, one takes the diffusion coefficient for the chemical stimulus transport to be significantly higher than one would expect simply from diffusion, as discussed further in Appendix A.1.

The cell is assumed to migrate as though it were a diffusing substance *far* from the wound edge, which is consistent with previous modelling strategies. We explicitly incorporate the wound edge in the model, where it is represented by a moving boundary, in the mathematical sense. One subsequently requires the specification of conditions that govern the boundary's movement, which we now motivate.

Experimental observations indicate that there is a well defined wound edge, which on the cellular side, consists of a continuous monolayer of corneal epithelial cells (Crosson *et al.*, 1986; Dua *et al.*, 1994). The implementation of a moving boundary requires knowledge of the cell density at this wound edge, and knowledge of the jump in the derivative of the cell density at this point. The latter is determined by a Rankine–Hugoniot condition (Elliot & Ockendon, 1982), which represents the fact that the cellular kinetics are continuous on the cellular side at the wound edge on approaching this edge, with no additional sink or

source of cells concentrated at the wound edge. This is a biologically reasonable condition in that no proliferation or desquamation of cells is observed at the wound edge once migration has started (Crosson *et al.*, 1986).

The specification of the cell density at the leading edge requires more care. Estimates of monolayer cell density based on the unwounded cornea can be *too high* due to increases in cellular volume (Dua *et al.*, 1994; Crosson *et al.*, 1986) and cell flattening in the healing corneal epithelium (Crosson *et al.*, 1986). In the modelling below, it is assumed that such effects are either absent or are transient; i.e. they occur only during the premigratory and very early migratory phases of the CEWH response. This is consistent with the observations of Crosson *et al.* (1986), where the above two effects were reported up until two hours after the start of cell migration during CEWH, but not after this point.

For the modelling below, we initially use estimates of monolayer cell density at the wound edge based on unwounded cornea data. We will also demonstrate that the conclusions of this paper are supported equally well when the modelling is performed with a reduction in the monolayer cell density at the wound edge. One may question whether the use of the continuum approximation below is valid at the wound edge, where there is only a monolayer of cells, but implicit in the continuum approximation for our model is that one is averaging the cell behaviour over the surface of the wounded eye. It does not hinge on averaging normal to the eye.

Further to simulating migration mechanisms, the model must incorporate sources and sinks of its constituents and simulate how they interact, as detailed below.

- The cells can also undergo mitosis, represented by a chemically stimulated logistic process, and can be desquamated, represented by an exponential decay.
- We assume a constant source of chemical stimulus present in the tear film. The chemical is assumed to decay with a half life of the order of the half life of epidermal growth factor, as this is the most common factor reported to regulate cellular processes during CEWH.

  It is also assumed that the cells internalize the chemical–receptor complex formed on the cell surface, which acts effectively as a cell-dependent chemical stimulus degradation process. In one of the realizations of the modelling framework we assume the presence of a wound bed source of chemical stimulus, in line with previous modelling efforts (Dale *et al.*, 1994a,b).

Finally, the model must capture the effects of the presence of an electric field.

- We assume that the presence of a physiological electric field affects only the migration of the cells. As depicted in Section 2.1 the physiological electric field will possess a heterogeneity in the vertical direction, i.e. the direction perpendicular to the basal lamina; see Fig. 1. However, we implicitly neglect such heterogeneity, and thus consider some average of the electric field over the vertical degree of freedom. Hence we are simply considering the cells migrating in a lateral field, which is of key interest biologically (Zhao *et al.*, 1996a,b,1997,1999a). This allows a reduction in the dimensions of the model; generalizations including the vertical heterogeneity of the electric field are briefly discussed in the conclusions. In line with the presentation of Zhao *et al.* (1996a,b) and the discussion in Section 2.1,

we assume the electric field imposes a drift directionality. Thus an individual cell can be considered to undergo an asymmetric random walk, which in the continuum limit yields a convective–diffusion process. Consequently, the resulting continuum equation contains a drift term, driven by the electric field, in addition to the usual diffusive term.

3.3 *Model framework equations*

Here we specify the equations of the modelling framework. Some functions are left undefined at this stage, and will vary between two different realizations of the modelling framework that will be considered below. The dimensionalized independent and dependent variables of the model, plus important functions of these, are labelled by

N: generic corneal epithelial cell density;
C: chemical stimulus concentration;
X: Cartesian coordinate, with $X = 0$ corresponding to outer (i.e. limbal) edge and $X = X_*$ corresponding to the centre of the cornea;
T: time (seconds);
$X_{mvb}(T)$: the position of the wound edge, i.e. the mathematical moving boundary, at time T.

When the above expressions occur with lower case letters in the following this refers to the nondimensionalized analogue. As the chosen nondimensionalization is slightly different from that adopted in previous modelling efforts, we consider this relatively tedious aspect of the model in detail below. The dimensionalized equations are, for $X < X_{mvb}$,

$$\begin{aligned}
\frac{\partial N}{\partial T} &= \nabla_X(D(C)\nabla_X N) + \nabla_X(E(X,T)N) + (\rho_* + \bar{\rho}_* C)\left(\varsigma_* N - \frac{N^2}{N_0}\right) - \frac{1}{T_*}N,\\
\frac{\partial C}{\partial T} &= D_{C*}\nabla_X^2 C + A_* + B(N) - \frac{\mu_* N C}{\hat{C} + C} - \delta_* C,\\
D(C) &= (\alpha_* + \bar{\alpha}_* C).
\end{aligned} \tag{1}$$

The function $B(N)$ is a wound bed source term; different choices of $B(N)$ will correspond to different realizations of the modelling framework below. The function $E(X, T)$ is proportional to the electric field and is discussed in detail in the subsequent sections.

Note that the model can support the homogeneous nontrivial steady state, i.e. the unwounded steady state; namely,

$$(C, N) = (C_{eqm} \equiv \text{ constant}, N_{eqm} \equiv \text{ constant}) \tag{2}$$

for given observed equilibrium values of (C_{eqm}, N_{eqm}), provided we take

$$A_* = -B(N_{eqm}) + \frac{\mu_* N_{eqm} C_{eqm}}{\hat{C} + C_{eqm}} + \delta_* C_{eqm}. \tag{3}$$

Further comment is required concerning the kinetics terms in equation (1) above. The first term represents chemically stimulated mitosis; the second term represents desquamation. The parameters ρ_* and $\bar{\rho}_*$ have a degree of scaling invariance, in that rescaling these parameters can be compensated for by rescaling ς_* and N_0. Hence, without loss of generality, we may set

$$\rho_* + \bar{\rho}_* C_{eqm} = \frac{1}{T_*}. \tag{4}$$

As discussed by Dale *et al.* (1994a,b), we may assume that the kinetic term in equation (1) reduces, at equilibrium chemical levels, to

$$\frac{1}{T_{dble}}\left(N - \frac{N^2}{N_{eqm}}\right), \tag{5}$$

where $\ln(2)T_{dble}$ is the doubling time of the corneal epithelium, i.e. the time in which, without cell loss, the corneal epithelium would produce it own mass. This expression must thus equal

$$\frac{1}{T_*}\left((\varsigma_* - 1)N - \frac{N^2}{N_0}\right) \tag{6}$$

for arbitrary values of N. Again we have a scaling invariance, and hence, without loss of generality, we may take

$$\varsigma_* = 2, \qquad N_0 = N_{eqm}, \qquad T_* = T_{dble}. \tag{7}$$

Note that in equation (1) we have that μ_* is a measure of the rate of internalization of chemical stimulus by the cells, as motivated in previous models of CEWH (Dale *et al.*, 1994a,b). We also have that δ_* gives the exponential decay rate of the chemical stimulus.

The initial conditions and boundary conditions that do not involve the moving boundary take the form

$$\begin{aligned} D\nabla_X N + EN = \nabla_X C = 0 \qquad & \text{at } X = 0, \\ \nabla_X C = 0 \qquad & \text{at } X = X_*, \end{aligned} \tag{8}$$

$$N(X, T=0) = \begin{cases} 0 & \text{if } X \in \text{initial wound}, \\ N_{eqm} & \text{if } X \notin \text{initial wound}, \end{cases}$$

$$C(X, T=0) = \begin{cases} 0 & \text{if } X \in \text{initial wound}, \\ C_{eqm} & \text{if } X \notin \text{initial wound}. \end{cases} \tag{9}$$

The condition on the cell density at $X = 0$ is one of zero flux, due to the notion that for nonpathological healing, conjunctival cells do not invade the cornea. This is the conclusion of the studies demonstrating that transdifferentiation at the outer edge of the cornea, i.e. the limbus, does not occur (Tseng, 1989). The chemical flux is also taken to be zero at $X = 0$ (Dale *et al.*, 1994b). The boundary condition at $X = X_*$ for the chemical is determined by the fact we take there to be a reflection symmetry in the line $X = X_*$, so that we need only

model half of the cornea, which is valid for a large class of possible corneal wounds and we restrict the modelling to this situation below.

The conditions which determine the moving boundary are as follows

$$N(X_{mvb}(T), T) = N_* = \text{constant},$$
$$\Big(D(C)\nabla_X N(X,T) + E(X,T)N(X,T)\Big)\Big|_{(X_{mvb}(T),T)} = -N_* \frac{\mathrm{d}X_{mvb}(T)}{\mathrm{d}T}, \qquad (10)$$

as motivated in Section 3.2. No conditions need be given for the chemical concentration at the moving boundary, and in Appendix B we demonstrate that $C(X,T)$ is twice continuously differentiable at the moving boundary given the existence, uniqueness, and boundedness of a solution which may have a jump discontinuity in both the chemical concentration and cell density at the moving boundary, but is continuous elsewhere.

3.3.1 *Nondimensionalization.* We nondimensionalize length scales with respect to the characteristic length of the cornea, X_*. Time scales are nondimensionalized using T_*. We have explicitly

$$X \to x = \frac{X}{X_*}, \qquad T \to t = \frac{T}{T_*}, \qquad N \to n = \frac{N}{N_{eqm}},$$
$$C \to c = \frac{C}{C_{eqm}}, \qquad N_* \to n_* = \frac{N_*}{N_{eqm}}, \qquad \alpha_* \to \alpha = \frac{T_*\alpha_*}{X_*^2},$$
$$\bar{\alpha}_* \to \bar{\alpha} = \frac{C_{eqm}T_*\alpha_*}{X_*^2}, \qquad \rho_* \to \rho = T_*\rho_*, \qquad \bar{\rho}_* \to \bar{\rho} = C_{eqm}T_*\bar{\rho}_*,$$
$$\varsigma_* \to \varsigma = \varsigma_* = 2, \qquad D_{C*} \to D_c = \frac{T_*D_{C*}}{X_*^2}, \qquad A_* \to A = \frac{T_*A_*}{C_{eqm}},$$
$$\hat{C} \to \hat{c} = \frac{\hat{C}}{C_{eqm}}, \qquad \delta_* \to \delta = T_*\delta_*, \qquad \mu_* \to \mu = N_{eqm}T_*\mu, \qquad (11)$$

$$E(X,T) \to e(x,t) = \frac{T_*}{X_*}E(X_*X, T_*T), \qquad B(N) \to b(n) = T_*B(N_{eqm}n).$$

3.3.2 *The electric field function, $e(x,t)$.* As discussed in Sections 2.1 and 2.2, the electric field is taken to exist in the wound bed and to penetrate the healing epithelium to a small skin depth not greater than 1 mm. As the skin depth cannot be estimated to greater precision, we initially take it to be smaller than the upper bound of 1 mm, and proceed to confirm in Section 5 that the conclusions presented are robust to variations in this parameter. We take the skin depth, denoted by Δ_*, to be given by

$$\Delta_* = 0.1X_*. \qquad (12)$$

As X_* is half the length scale of a cornea and, as discussed below, taken to be 8 mm (Forrester *et al.*, 1996) this gives Δ_* to be 0.8 mm, corresponding to a nondimensionalized skin depth of

$$\Delta = 0.1. \qquad (13)$$

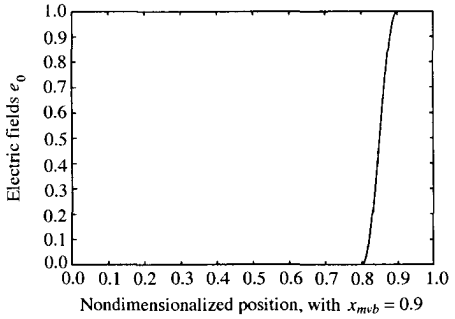

FIG. 2. An electric field profile for the model, with a smooth interpolation within the skin depth region, where the electric field persists in the presence of cells.

We thus model the electric field by

$$e(x,t) = \begin{cases} 0 & \text{if } x \in [0,\ x_{mvb}(t) - \Delta], \\ e_0 \times 0.5\left\{1.0 + \sin\left[\dfrac{\pi}{2}\left(\dfrac{2.0(x - (x_{mvb}(t) - \Delta))}{\Delta} - 1.0\right)\right]\right\} & \text{if } x \in (x_{mvb}(t) - \Delta, x_{mvb}(t)), \\ e_0 & \text{if } x \in [x_{mvb}(t),\ 1]. \end{cases} \tag{14}$$

The sine function yields a monotonic smooth interpolation between where the electric field is zero and where it takes the value e_0. A typical plot of the electric field is presented in Fig. 2.

Unfortunately, estimating the magnitude of e_0 from experimental data is difficult. This is because the convective term in the equations representing the effect of the electric field represents a contribution to the limit of an asymmetric random walk, and the value of this limit is undetermined by this formalism, much in the same way that a diffusion coefficient is left undetermined. Consequently, the constant of proportionality between the electric field and the function $E(X,T) = (X_*/T_*)e(x,t)$ is unknown. (There are two possibilities for determining the value of e_0. One is to determine the relationship between e_0 and microscopic data, available in the literature (Zhao *et al.*, 1996a,b). This can be performed via a generalization of the work of Dickinson & Tranquillo (1995), where such a link is forged in other systems by averaging over rapid timescales of suitable stochastic differential equations representing the microscopic motion. The other alternative is to predict e_0 by comparing observations of the macroscopic system with modelling results.)

At this stage, we leave e_0 undetermined, and present the results in terms of the variation of e_0 which leads to a change in the wound healing speed by a factor of approximately three. This may realistically be taken to constitute a physiologically large range for the electric field strength.

3.3.3 *The wound bed source function, $b(n)$.* MODEL I In the modelling below, we consider the possibility of wound healing without stimulus being produced in the wound bed. This represents a particular realization of the above modelling framework, which we

denote by model I and for which we simply set

$$b(n) = 0. \tag{15}$$

MODEL II We will find, as in previous modelling efforts (Dale *et al.*, 1994a,b), that modelling without the presence of a wound bed source will result in predictions for wound healing rates that are too low. Not surprisingly, a wound bed source increases the healing rates, and can be motivated from experimental evidence too (Barrandon & Green, 1987; Dunn & Ireland, 1984), so we include such a source in a second realization of the modelling framework, denoted as model II.

We take the size of the wound bed source to be that required to bring the wound healing speeds up to experimentally observed levels of approximately $60\mu\text{m h}^{-1}$ (Crosson *et al.*, 1986). We will see below that such a level of a wound bed source is of the order of the tear film source term and so is not unreasonably high. The fact we fix this parameter somewhat artificially does not detract from the conclusions of this paper, which are robust to such changes in the different realizations of the modelling framework, as will be seen below.

To include a wound bed source term, we take $b(n)$ to be of the form

$$b(n) = \begin{cases} 0 & \text{if } x \in (0,\ x_{mvb}(t)), \\ \psi & \text{if } x \in (x_{mvb}(t),\ 1), \end{cases} \tag{16}$$

where ψ is chosen so that the wound healing speed, in the absence of the electric field, is roughly that which is experimentally observed, namely $60\mu\text{m h}^{-1}$. Strictly one should account for the presence of a small physiological electric field when performing such a normalization of ψ. This cannot be done due to problems in estimating e_0. However, the model robustness, as illustrated in Section 5, ensures that the model conclusions are nonetheless valid.

We will demonstrate that the general trends observed concerning the variation of the wound healing speed with the electric field hold for both realizations of the modelling framework, indicating that the near-linear relation between the electric field strength and the wound healing speed derived in this paper holds in quite a general setting.

3.3.4 *Nondimensionalized equations.* In summary, the above equations thus reduce to the form

$$\begin{aligned}
\frac{\partial n}{\partial t} &= \nabla_x((\alpha + \bar{\alpha}c)\nabla_x n) + \nabla_x(e(x,t)n) + (\rho + \bar{\rho}c)(2n - n^2) - n, \\
\frac{\partial c}{\partial t} &= D_c \nabla_x^2 c + A + b(n) - \frac{\mu n c}{\hat{c} + c} - \delta c, \\
\nabla_x n &= \nabla_x c = 0 \quad \text{at } x = 0, \\
\nabla_x c &= 0 \quad \text{at } x = 1, \\
n(x, t=0) &= \begin{cases} 0 & \text{if } x \in \text{initial wound}, \\ 1 & \text{if } x \notin \text{initial wound}, \end{cases} \\
c(x, t=0) &= \begin{cases} 0 & \text{if } x \in \text{initial wound}, \\ 1 & \text{if } x \notin \text{initial wound}, \end{cases}
\end{aligned} \tag{17}$$

with the moving boundary conditions

$$n(x_{mvb}(t), t) = n_* = \text{constant},$$
$$\{[\alpha + \bar{\alpha}c(x,t)]\nabla_x n(x,t) + e(x,t)n(x,t)\}|_{(x_{mvb}(t),t)} = n_* \frac{\mathrm{d}x_{mvb}(t)}{\mathrm{d}t}. \tag{18}$$

The function $e(x,t)$ is given by (14) while $b(n)$ is given by (15) or by (16) for the realizations of the modelling frameworks of model I or model II, respectively.

3.3.5 *Parameter estimation.* The parameters used in the modelling are given in Appendix A unless explicitly stated otherwise. The routine parameter estimation is performed in Appendix A.1. Here, we consider aspects of parameter estimation that are particularly important in that they highlight areas where parameters in the model may not be pinned down. It is crucial to confirm the robustness of the model in such situations, which motivates the robustness investigation of Section 5.

We first of all consider aspects of the initial conditions. A linear scale of half a cornea is represented by X_*, as we implicitly have a reflection symmetry about $x = 1$ in our equations. Thus X_* is taken to be 0.8 cm, as the diameter of a (human) cornea is typically ~ 1.6 cm (Forrester *et al.*, 1996). We simulate the equations for the closure of a large (a substantial wound was chosen to be modelled in preference to a small wound so that any trends exhibited by the model data would be as explicit as possible, without risk of being obscured by any possible initial transients), rectangular initial wound with a length of $0.5X_*$ on its shorter edge and a substantially larger longer edge (e.g. a length of $\sim 1.2X_*$). The wound edge migration in the model is taken to represent the migration of the experimental wound's longer edge, near its centre. As we are modelling half of a symmetric system, centred at $X = X_*$, such an initial wound corresponds to taking the model's initial wound in the region $X > 0.75X_*$, or $x > 0.75$. Clearly though, it is important to consider variations of the initial wound size when considering robustness.

Investigating robustness is also important for parameters which are difficult to estimate, such as N_*, the cell density of the monolayer of the healing cornea epithelial wound. The estimation of this parameter is difficult, as discussed in Section 3.2, and estimates based on unwounded corneal data are likely to be too high. We will initially work with an unwounded estimate. This is the cell density of a single layer of cells in the unwounded central cornea; as there are five cell layers in the central cornea (Dua *et al.*, 1994), we thus initially take

$$N_* = 0.2N_{eqm} \quad \text{i.e. } n_* = 0.2. \tag{19}$$

We also investigate the model with $N_* = 0.1N_{eqm}$, i.e. $n_* = 0.1$, which will demonstrate that the conclusions from this modelling are still supported on reduction of N_* from its upper bound used in equation (19).

As discussed in Section 3.3.2, we take $\Delta = 0.1$. From the discussion of Section 2.1, the electric field penetration into the corneal epithelium is not more than 1 mm, giving an upper bound for Δ of 0.125. As Δ is only constrained by an upper bound, we also investigate variations of Δ in Section 5.

4. Results

A brief description of the numerical algorithm used to solve the above equations is given in Appendix A.1. In the results presented in this section, the initial wound is always taken be in the region $x > 0.75$.

The parameters that will vary between the various runs in this section are

$$\psi, \qquad e_0. \tag{20}$$

Variations of Δ, n_*, and the size of the initial wound will be considered in Section 5.

4.1 *Individual run results*

In this section we present some sample profiles of cell densities, chemical concentrations, and electric fields from individual runs of the model.

4.1.1 *Model I, no electric field (see Fig. 3).* In Fig. 3, results are presented for model I with no electric field. Note that the chemical concentration undergoes a very rapid initial change. This occurs on a timescale much faster than the timescale of change of the cellular density as the chemical diffusion coefficient is much greater than the cell diffusion coefficient. Note that after initial transients the moving boundary settles down to an approximately constant speed in Fig. 3.

4.1.2 *Model I, positive electric field (see Fig. 4).* In Fig. 4 results are presented for model I in the presence of a large positive electric field. The same comments made for the zero electric field apply here also, except that, obviously, the plots of the electric field are no longer trivial. In addition, note that the wound healing occurs at a much slower speed. The variation of the speed with the electric field will be investigated further.

4.1.3 *Model I, negative electric field (see Fig. 5).* In Fig. 5, results are presented for model I with a large negative electric field. The comments made concerning Fig. 3 also apply for Fig. 5. The features displayed in Fig. 5 are qualitatively the same as those displayed by plots for the other model realizations and for different parameters. Hence, such plots are not shown.

Obviously, one would prefer to be able to approximate the speed of the moving boundary in some large time limit. For linear kinetics one can derive such an approximation for moving boundary problems, with one dependent variable at least, by considering the Laplace transformed equations (Elliott & Ockendon, 1982). The presence of nonlinear kinetics prevents such an approach; as no standard approach seems to be valid for such equations, the investigation of possible alternatives is being actively pursued (Gaffney, 1999).

4.2 *Detailed investigation of the speed of the moving boundary*

The most interesting aspect of the model framework presented is the simple relationship of the variation of the wound healing speed with the electric field strength, which, as we will see, is robust. In this section, the nature of this relationship is illustrated.

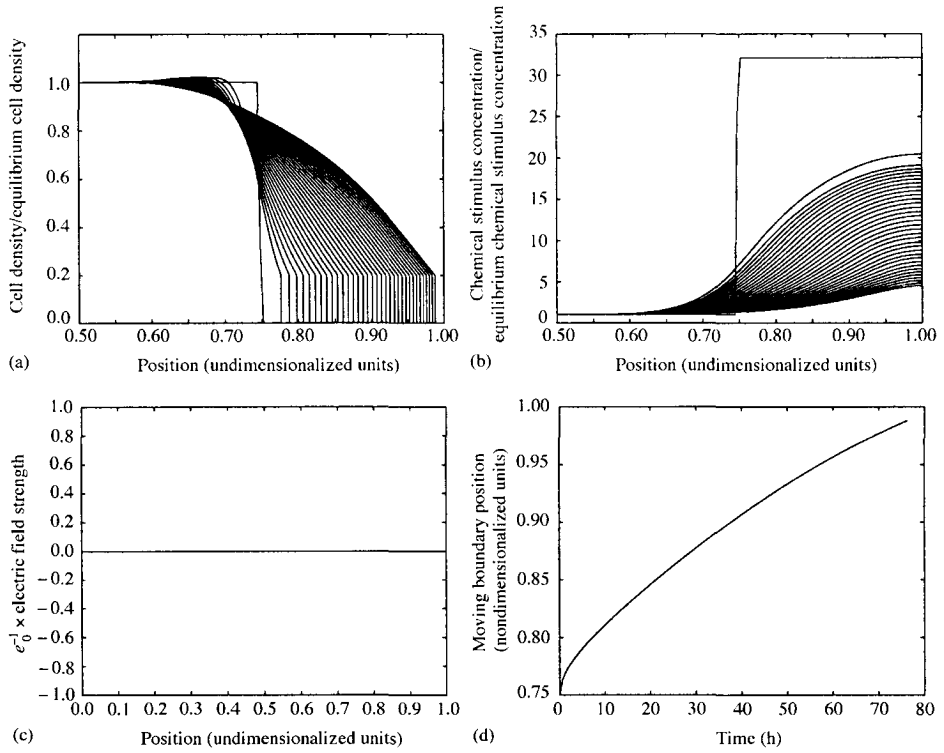

FIG. 3. Model results for zero electric field, with $e_0 = 0$, $\Delta = 0.1$, $n_* = 0.2$ and no wound bed source; i.e. $\psi = 0$. The other parameters are as listed in Appendix A.1. Plots every 2.2 h of: (a) the cell number density, (b) the chemical concentration, and (c) the electric field strength. (d) The position of the moving boundary as a function of time. Due to the symmetry assumptions, the above graphs show the wound closing, with the mirror image of the cell density on reflection in the line $x = 1$ approaching $x = 1^+$ as the moving boundary depicted in (c) approaches $x = 1^-$.

4.2.1 *Model I, wound healing speed investigation (see Fig. 6).* In Fig. 6 various plots are presented for model I. Figure 6(a) represents the wound healing profile after initial transients, on a time–space plot. The top left line in Fig. 6(a) corresponds to an electric field of strength -0.625 in normalized units, and the bottom right line corresponds to an electric field of strength 0.625 in normalized units. As discussed at the end of Section 3.3.2, the difficulties in estimating e_0 imply that we cannot actually determine the electric fields corresponding to such normalized electric field values. However, Fig. 6 does show how the wound healing process may change as one varies the electric field for a large physiological range.

Figure 6(b)–(c) study aspects of the first graph in more detail. Figure 6(b) gives the average wound healing speed, after initial transients. What is noteworthy is its linearity, especially given the wide range of speeds over which it is considered. Figure 6(c) quantifies the deviation of the actual moving boundary from a hypothetical boundary, with the average speed as plotted in Fig. 6(b), and the same initial start point. Away from initial

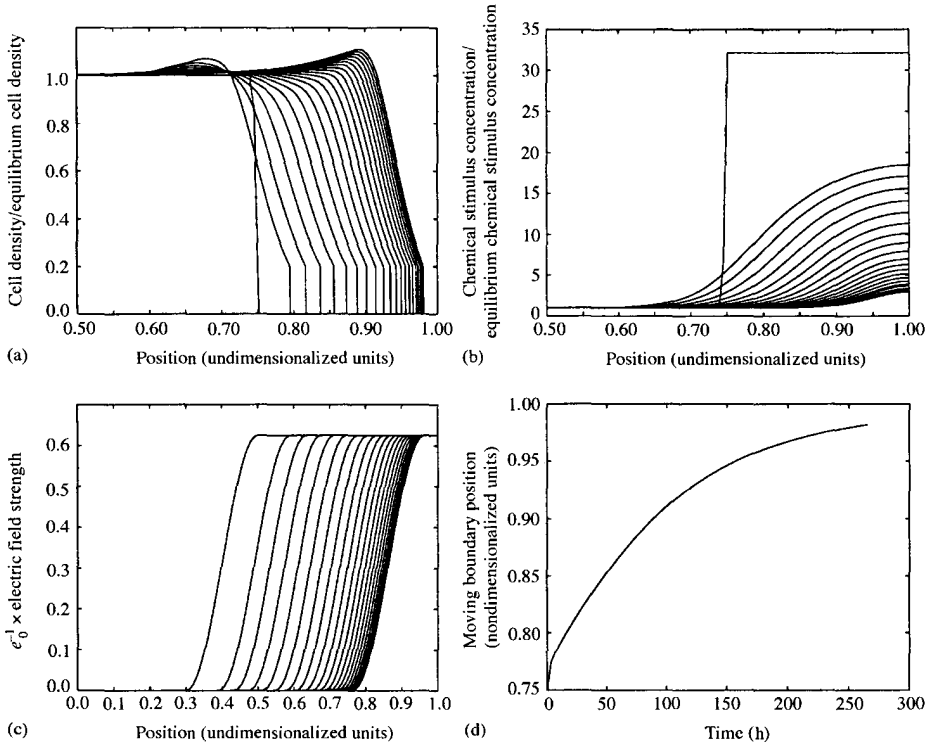

FIG. 4. Model results for a large positive electric field, with $e_0 = 0.625$, $\Delta = 0.1$, $n_* = 0.2$, and no wound bed source; i.e. $\psi = 0$. The other parameters are as listed in Appendix A.1. Plots every 13.1 h of: (a) the cell number density, (b) the chemical concentration, and (c) the electric field stength. (d) The position of the moving boundary as a function of time.

transients, the following measure of deviation is calculated

$$\frac{|X_{mvb}(T) - \{X_{mvb}(T_0) + T * [\text{speed from Fig. 6(b)}]\}|}{\text{initial wound size}}, \tag{21}$$

where $T_0 \sim 6$ h is the first time plotted in Fig. 6(a). The mean average of this quantity is plotted in Fig. 6(c). One can see that for negative electric field strengths the agreement between a hypothetical boundary with the average speed and the moving boundary is good, being less than 10%. Unsurprisingly, the deviation increases with increasing electric field, though it still yields a rough order of magnitude approximation for the behaviour of the moving boundary for the variation of wound healing speeds considered. The manner of the deviation from the average speed is clear from Fig. 6(a), where the wound edge is seen to decelerate significantly at large positive electric fields.

4.2.2 *Model II, wound healing speed investigation (see Fig. 7).* In Fig. 7 results from an investigation of the moving boundary's speed are presented for model II. The layout and format of the graphs is the same as those presented for Model I in Fig. 6. Figure

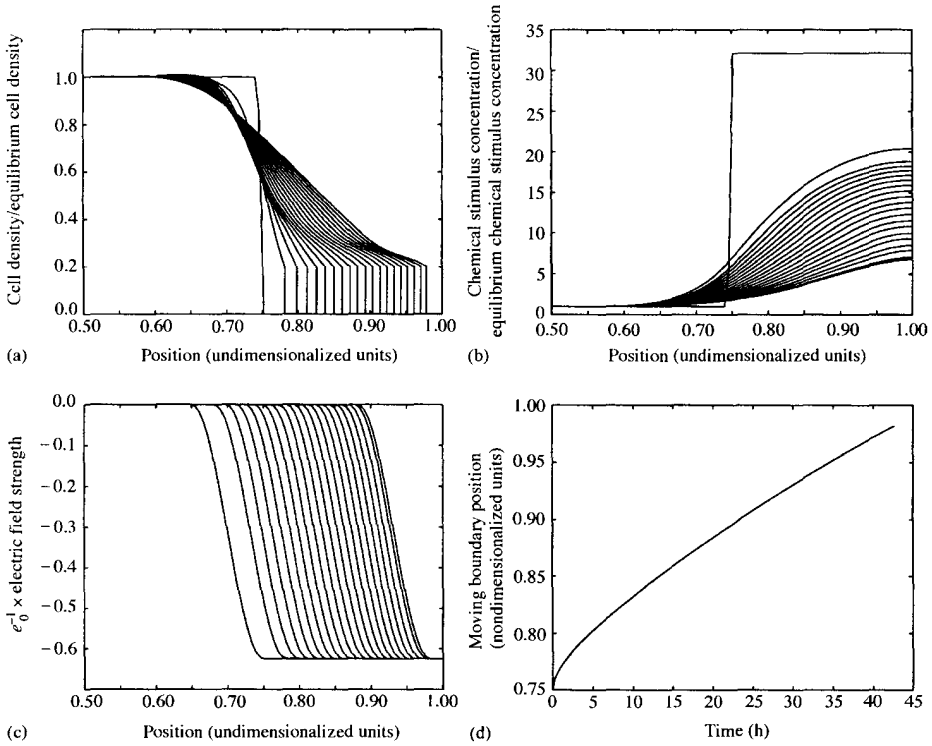

FIG. 5. Model results for a large negative electric field, with $e_0 = -0.625$, $\Delta = 0.1$, $n_* = 0.2$, and no wound bed source; i.e. $\psi = 0$. The other parameters are as listed in Appendix A.1. Plots every 2.2 h of: (a) the cell number density, (b) the chemical concentration, and (c) the electric field strength. (d) The position of the moving boundary as a function of time.

7(a) represents the wound healing profile after initial transients, on a time–space plot, for various electric fields strengths. Figure 7(b) gives the average wound healing speed, after initial transients. Again, its linearity is noteworthy. Fig. 7(c) is a plot of (21), using the speed from Fig. 7(b); the comments made for model I also apply.

4.2.3 *Conclusions from the above results.* Two key points emerge from the graphs.

- Over a (physiologically) large variation of the electric field strength, the model predicts that, after initial transients, the average wound healing speed varies linearly with the electric field to a good approximation. This holds for both models I and II.
- Both model I and model II indicate that, away from initial transients, a constant speed approximation to the moving boundary yields an order of magnitude estimate for the position of the model's wound edge. This approximation is actually very good for negative electric field strengths.

It should be noted that for extremely large, positive, electric fields the above conclusions break down, though such results are not displayed. In such situations the wound edge stalls

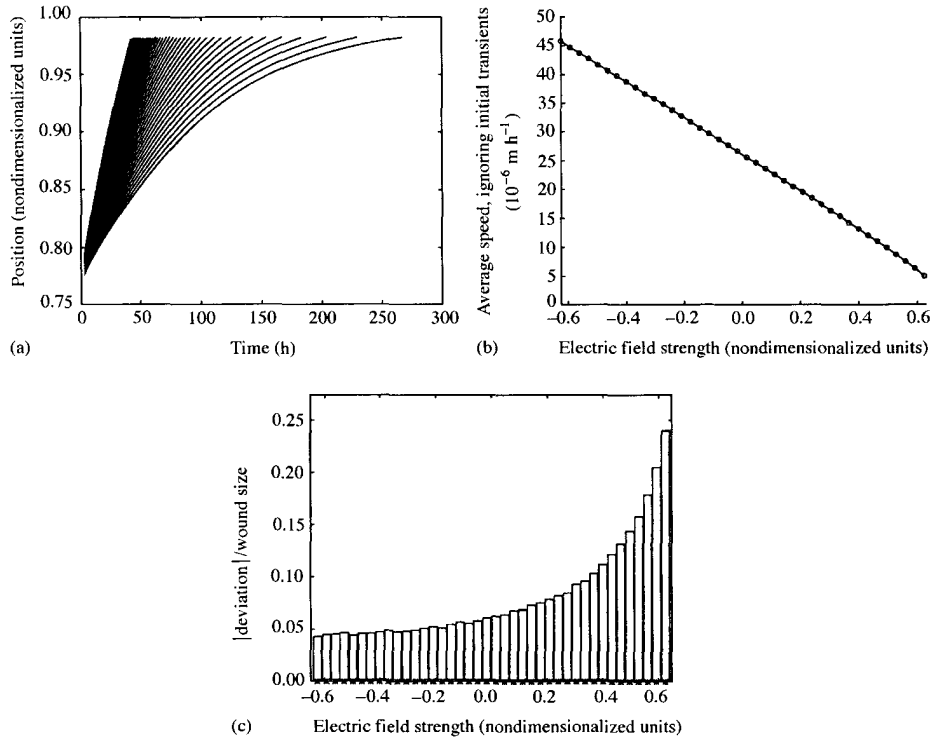

FIG. 6. Graphs detailing the nature of the moving boundary's position in time with various electric field strengths for model I. We have $\Delta = 0.1$, $n_* = 0.2$, and no wound bed source, i.e. $\psi = 0$, while the other parameters are as listed in Appendix A.1. (a) The wound healing profile after initial transients, on a time–space plot. The line in the top left corresponds to an electric field of strength −0.625 in normalized units and the line in the bottom right corresponds to an electric field of strength 0.625 in normalized units. (b) The average wound healing speed, after initial transients. (c) A quantification of the deviation of the actual moving boundary from a hypothetical boundary with the average speed plotted in Fig. 6(b), and the same initial start point. See the text for details.

in the model predictions. It is not clear whether the model predicts that the wound edge would subsequently move backward after stalling owing to limitations of the numerical algorithm, which cannot track a change in direction of moving boundary without further work. However, such large electric fields are not relevant to the biological situation, so this breakdown of the conclusions above occurs in a regime far outside that of biological interest, and is thus neglected elsewhere in this paper.

5. Comments on robustness

As discussed in Sections 3.2 and 3.3.5, we are unsure of the numerical value of n_*, or equivalently N_*. We have used an estimate for n_* based on unwounded equilibrium considerations, which yields $n_* = 0.2$, but this is likely to be too high. The conclusions drawn in Section 4.2.3, however, hold even more emphatically on reducing n_*.

With $n_* = 0.1$, results are presented in Fig. 8 for model I, i.e. with no wound bed

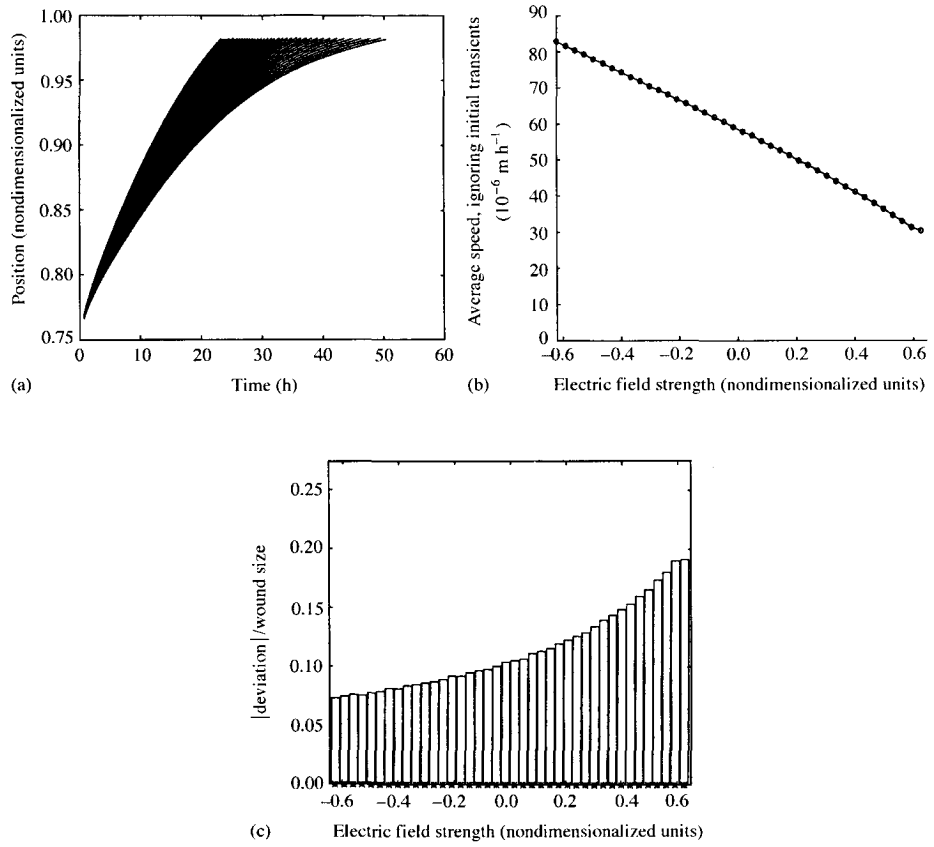

FIG. 7. Graphs detailing the nature of the moving boundary's position in time with various electric field strengths for model II. We have $\Delta = 0.1$, $n_* = 0.2$ and a wound bed source with $\psi = 2A$, while the other parameters are as listed in Appendix A.1. (a) The wound healing profile after initial transients, on a time–space plot. The line in the top left corresponds to an electric field of strength -0.625 in normalized units, and the line in the bottom right corresponds to an electric field of strength 0.625 in normalized units. (b) The average wound healing speed, after initial transients. (c) A quantification of the deviation of the actual moving boundary from a hypothetical boundary with the average speed plotted in the second graph, and the same initial start point (see equation (21) and the discussion in text).

source $\psi = 0$. Again, the layout and format in Fig. 8 is the same as in Fig. 6 and 7. The linearity of the wound healing speed after initial transients is again noteworthy, in Fig. 8(b). Figure 8(c) is a plot of equation (21), using the speed from Fig 8(b). This represents the deviation of the model moving boundary from a hypothetical moving boundary with the speed, for a fixed electric field strength, given in Fig. 8(b). Note that the deviation is lower than that presented in either Fig. 6 or Fig. 7. One can easily see that the conclusions of Section 4.2.3 apply to these results too.

Exactly the same conclusions hold on considering the results for model II with $n_* = 0.1$ and, as discussed in Appendix A.1, with $\psi = A$. The results (not shown) are analogous to Fig. 8 except that the deviations from a linear relation between wound healing speeds

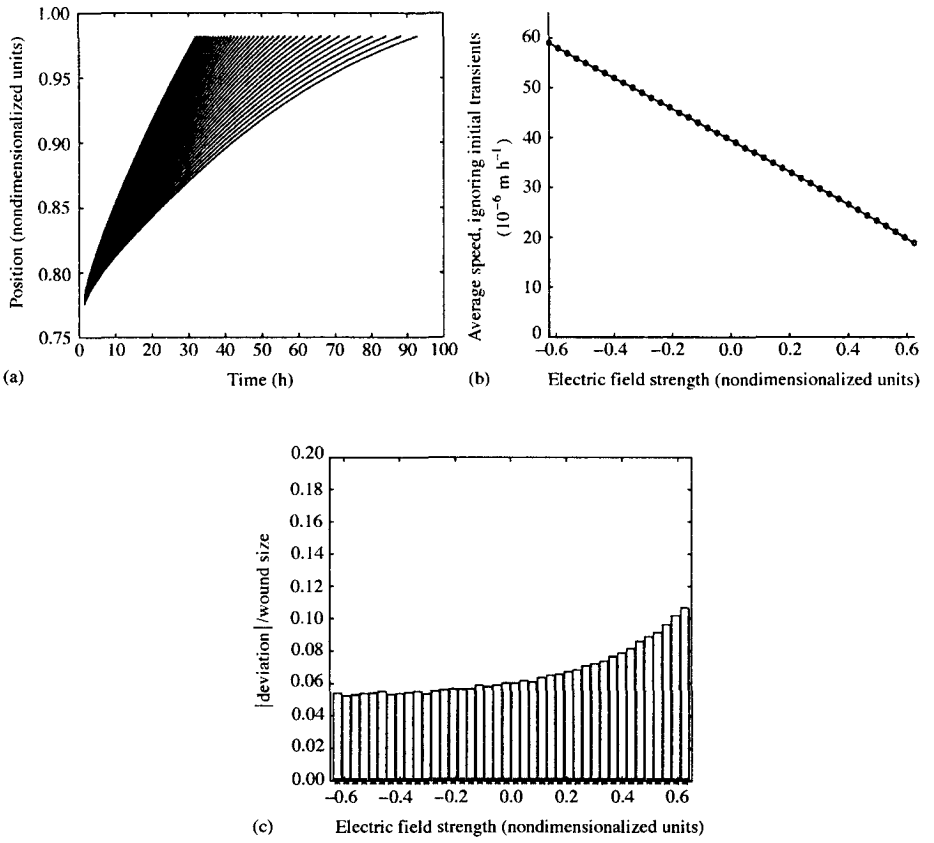

FIG. 8. Graphs detailing the nature of the moving boundary's position in time with various electric field strengths for model I with, importantly, *a reduced value of* n_*; here taken to be $n_* = 0.1$ (that is, the cell density at the moving boundary is eual to $0.1N_{eqm}$). We also take $\Delta = 0.1$, with the other parameters values as listed in Appendix A.1. (a) The wound healing profile after initial transients, on a time–space plot. The line in the top left corresponds to an electric field of strength -0.625 in normalized units, and the line in the bottom right corresponds to an electric field of strength 0.625 in normalized units. (b) The average wound healing speed, after initial transients. (c) A quantification of the deviation of the actual moving boundary from a hypothetical boundary with the average speed plotted in the second graph, and the same initial start point (see equation (21) and the discussion in text).

and electric field strengths is further reduced. The above has been investigated for the same relative variation of the wound healing speed, i.e. such that the range of variation in e_0 results in the same relative variation of the wound healing speed typically displayed above.

One finds analogous results, in that the conclusions stated in Section 4.2.3 hold, on variation of the parameter Δ. This has been confirmed on increasing Δ beyond its upper bound of $\Delta = 0.125$, and also on using $\Delta = 0.05$, which is half the value used above. Again, this is for the same relative variation of the wound healing speed. It has also been confirmed that the conclusions of Section 4.2.3 hold on considering a smaller initial wound and on varying the parameter D_C which is difficult to estimate, as detailed in Appendix

A.1. Thus we have an additional and very important conclusion that:

- the linear relation between the average wound healing speed away from initial transients and the electric fields strength appears to be extremely robust.

6. Discussion and conclusions

A moving boundary formalism has been used to investigate the modelling of corneal epithelial wound closure, especially in the presence of an electric field. Key conclusions to be drawn from the modelling are given in Section 4.2.3. The most important of these is that, after initial transients, the average wound healing speed varies linearly with the electric field strength over a physiologically large range (as discussed at the end of Section 3.3.2). Even more important is the further conclusion that this relation is very robust. It is not invalidated by variation of the parameters, including variations of n_* and Δ which are difficult to estimate precisely, and also variation of the wound size. Furthermore, it does not break down on examining different realizations of the modelling framework, such as whether or not one includes a wound bed source term. Such key model predictions provide a potential insight into the manner in which an electric field could affect the wound healing response of corneal epithelium; clearly though, this is an area that requires further investigation, especially given the relative simplicity of the model used.

In terms of future possibilities, it would be interesting and informative to model interactive effects between electric fields, extracellular matrix elements and cells. Also, one would hope to be able to incorporate vertical heterogeneity of the electric field into the model. To predict the electric field in the vicinity of the healing corneal epithelial wound, one might attempt to use electrophysiology theory to yield the electric potential via a Poisson equation with an appropriate charge density source (on assuming that any magnetic field variation is negligible). This would provide a sufficient background, in theory, to enable a simulation of the vertically heterogeneous system, though one would have to carefully justify any continuum approximations or, perhaps, use discrete modelling in such a situation.

The model is not yet sufficiently well developed to start to influence experimental directions, though work is in progress to develop the model and its possible extensions to the extent that it can make testable predictions. For example, extensions of the model with multiple slit or ring wounds are in development. Further development of the modelling framework to encompass wound shapes that are genuinely two dimensional should also be considered. Such generalizations may offer predictions that will test how well different healing patterns observed clinically can correlate to model prediction. They will also provide insight into the extent to which experimental manipulation of the wound shape will change the local electric field patterns and hence the healing wound shape pattern.

The study of the effects of electric fields on the resulting pattern of wound healing is relevant from an experimental and clinical perspective in that its aim is to understand and clarify the involvement of physiological wound electric fields as one of the guidance and stimulating cues important for nonpathological wound healing. Indeed, evidence is accumulating which suggests that such electric fields have an important role in wound healing. We have: (i) there are physiological wound electric fields at the healing corneal wound (Chiang *et al.*, 1992), (ii) corneal epithelial cells respond to electric fields of

physiological strength by directional migration (Zhao *et al.*, 1996a,b,1999b), and (iii) *in vitro* corneal wound healing can be significantly modified by applying d.c. electric fields of the order of magnitude used in tissue culture studies (Sta Inglesia & Vanable, 1998). A further possibility for such work is the potential exploitation of the effects of electric fields on cell behaviours in the healing process. This will include, for example, modification of the electrical properties of a contact lens or an artificial cornea.

In summary, we have demonstrated the use of a moving boundary formalism for a model of corneal epithelial wound healing wound, with the motivation arising from biological necessity, rather than mathematical expediency. This has firstly led to a simple and robust prediction for the relationship between the electric field strength and the wound healing speed. The work presented here lays the foundation for future more detailed work studying the modelling of corneal epithelial wound healing in the presence of physiological electric fields, which has substantial potential for further application. More generally, we have illustrated how the moving boundary approach may be used for the modelling of invasive phenomena in biomathematical studies.

Appendix A: Parameter values

Parameter	Meaning	Value
X_*	$\frac{1}{2}$ length scale of cornea	0.8 cm
$\ln(2)T_*$	Average corneal replacement time	7 days
$N_0 \equiv N_{eqm}$	Average cell density	$(10^5)^3$ cells m^{-3}
N_*	Average cell density at wound edge	$\sim 0.2N_{eqm}$
C_{eqm}	Average chemical stimulus concentration (unwounded)	7×10^{-10} M
α	Coefficient for stimulus independent cell diffusion	0.012
$\bar{\alpha}$	Coefficient for stimulus dependent cell diffusion	0.2α
ρ	Coefficient for stimulus independent cell mitosis and differentiation	0.9
$\bar{\rho}$	Coefficient for stimulus dependent cell mitosis and differentiation	0.1
D_c	Stimulus diffusion coefficient	6.0
μ	Strength of chemical internalization by cells	2.0×10^4
$\hat{c}$	Parameter for cell–chemical internalization by cells	3.0
δ_*	Halving time of chemical stimulus	$1\ h^{-1}$
A	Strength of tear film chemical stimulus source	$0.25\mu + \delta$
$b(0) \equiv \psi$	Strength of wound bed source term	$\sim O(0.25\mu + \delta)$
e_0	Electric field strength	Not known (see Section 3.3.2)
Δ_*	Skin depth of electric field penetration	0.1

A.1 *Estimation of the parameters*

Typically in biological systems precise parameter estimation is difficult or impossible, though one can often deduce the order of magnitude of various parameters from experimental data. Here, we consider the parameter values used in this paper, which are those tabulated above, unless explicitly stated otherwise. Due to the use of a different convention for the nondimensionalization of length and timescales used below and in previous papers, the numerical values quoted below for some of the nondimensionalized versions of the variables tabulated above may differ from those used in previous papers.

Estimation of N_* and Δ are troublesome, and highlight areas for the investigation of robustness; consequently their estimation has already been considered in Section 3.3.5.

Now X_* represents a linear scale of half a cornea, and thus X_* is taken to be 0.8 cm, as the diameter of a (human) cornea is typically $\sim$ 1.6 cm (Forrester *et al.*, 1996). As we have seen above, $(\ln 2)T_*$ is the average doubling time, i.e. the time in which, without cell loss, the cornea would produce its own mass, or, equivalently, the time for the corneal epithelium to be renewed in the presence of cell loss. Dua *et al.*'s (1994) estimate is that this doubling time is between seven and ten days. For definiteness, we take

$$T_* = \frac{1}{\ln(2)} 7 \text{ days}. \tag{A1}$$

Of course, as both proliferative and quiescent cells are grouped into the N cell compartment, the actual cell doubling time of any cell capable of proliferation in the cornea is much less than T_*. The above value is slightly different from the value used by Dale *et al.* (1994a,b), as it is based on a more recent data source.

An order of magnitude estimate for $\alpha + \bar{\alpha}$ is performed by Gaffney *et al.* (1999) and yields, for the above nondimensionalization, $\alpha + \bar{\alpha} \sim 0.012$. From nondimensionalization we have $\rho + \bar{\rho} = 1$. We take the ratios $\alpha/\bar{\alpha}$ and $\rho/\bar{\rho}$ to be the same as those used by Dale *et al.* (1994a,b), which fixes α, $\bar{\alpha}$, ρ, and $\bar{\rho}$.

Using the fact that a typical cell length is about 10^{-5} m (Klyce & Beuerman, 1988; Dale *et al.*, 1994a,b), we have $N_0 \equiv N_{eqm} \sim 10^{15}$ cells m^{-3}. Now D_C* is difficult to experimentally measure, though it may be theoretically estimated to be $\sim 10^{-6}$ cm^2 s^{-1} (Berg & Von Hippel, 1985), which corresponds to $D_C \sim 1$. However, it is likely that any stimulus may be transported by many means other than just tear fluid diffusion within the cornea. Such mechanisms could include, for example, convection in the tear fluid flows and mixing due to blinking. Hence larger values for D_C are more realistic for the modelling of corneal epithelial wound healing, and we take $D_C \sim 5$. (One can confirm robustness to alterations in D_C, as mentioned in Section 5, provided the ratios between D_C and the cell diffusion coefficient are large, greater than $\sim$ 10; this will affect wound healing speeds and thus require an adjustment of the parameter ψ for model II, as described below equation (16). However, there is still a linear relationship between the electric field strength and the wound healing speed; thus the main conclusions, as summarized in Section 6, remain unchanged.)

The value of A is taken to be $\mu/4 + \delta$ for consistency (as by Dale *et al.*, 1994a,b), so that the nondimensionalized unwounded central corneal stimulus has the value 1.0. The estimation of μ is performed by Dale *et al.* (1994a,b), where for the nondimensionalization of this paper, one finds that $\mu \sim 2 \times 10^5$. Now $\hat{c}$ is estimated as by Dale *et al.* (1994a,b), and is found to be roughly 3.0. Dale *et al.* (1994a,b) speculated that $\psi \equiv B(0) \sim A$, though one may take ψ to be significantly larger without contradiction of any experimental data, though this is not required for the models in this paper. As discussed in Section 3.3.3 for realizations of the modelling framework with a wound bed source, we fix ψ so that the wound healing rate matches that which is experimentally observed. This does not detract from our aim of investigating the relation of wound healing speeds and the size of

the electric field. Hence we take

$$\psi = 2A \qquad \text{(model II; } N_* = 0.2N_{eqm}\text{)},$$
$$\psi = A \qquad \text{(model II; } N_* = 0.1N_{eqm}\text{)}.$$

Appendix B: On the regularity of $c(x, t)$

We deal with the nondimensionalized form of the equations (see Section 3.3.4), and show that $c(x, t)$ is twice continuously differentiable at the moving boundary, given the existence, uniqueness, and boundedness of a weak solution, which may have a jump discontinuity in both the chemical concentration and cell density at the moving boundary, but is otherwise smooth.

Suppose that a *weak* solution exists, is unique, bounded, and is given by $\{n(x, t), c(x, t), x_{mvb}(t)\}$, where one anticipates, at worst, jump discontinuities when $(x, t) = (x_{mvb}(t), t)$ and the corresponding singularities in the derivatives.

The c equation is of the form

$$\frac{\partial c}{\partial t} = D_c \frac{\partial^2 c}{\partial x^2} + f(x, t, n, c).$$

Setting $g(x, t) = f(x, t, n(x, t), c(x, t))$ and assuming the uniqueness of solutions of *both* the moving boundary problem and the scalar partial differential equation

$$\frac{\partial c}{\partial t} = D_c \frac{\partial^2 c}{\partial x^2} + g(x, t) \tag{B1}$$

gives $c(x, t)$, constituting part of the solution of the moving boundary problem, which solves (B1). Thus, for a suitable Green's function $G(x, t, x', t')$, we have for $t > 0$

$$\begin{aligned} c(x, t) &= \int_0^1 dx' G(x, t, x', 0) c_0(x') + \int_0^t dt' \int_0^1 dx' G(x, t, x', t') g(x', t') \\ &= \int_0^1 dx' G(x, t, x', 0) c_0(x') + \int_0^t dt' \int_0^{x_{mvb}(t')} dx' G(x, t, x', t') g(x', t') \\ &\quad + \int_0^t dt' \int_{x_{mvb}(t')}^1 dx' G(x, t, x', t') g(x', t'). \end{aligned} \tag{B2}$$

By assumption, $g(x, t)$ may have a jump discontinuity for $(x, t) = (x_{mvb}(t), t))$, but is continuous elsewhere, and thus $g(x't')$ is continuous for the range of integrations in the second and third integrals of (B2). This is sufficient to invoke the smoothness properties of the Green's functions to immediately deduce that $c(x, t)$ is twice continuously differentiable with respect to x: one simply applies Theorems 2–4 given by Friedman (1964, Sections 1–3) to the latter two integrals of (B2). Analogously, applying Theorem 5 shows that $c(x, t)$ is continuously differentiable with respect to time. This shows, given the above assumptions, that $c(x, t)$ satisfies its partial differential equation in a classical sense.

Appendix C: Overview of numerical algorithm

The algorithm used to numerically solve for the moving boundary is essentially that described in Crank's book (1987, Ch. 5). The chemical concentration is determined at each timestep via an explicit method, as is the cell density away from the moving boundary. Interpolations consistent with the equations yield the cell density near the moving boundary, as discussed by Crank (1987).

The algorithm has been improved slightly, in that the grid is not uniform, with a greater density of meshpoints in and near the initial wound bed. This ensures algorithm performance is quite sufficient for the needs of this paper.

It should be noted that some smoothing is added to the initial conditions to prevent algorithm difficulties due to the artefact that the model, as formulated above, presents a discontinuity at the initial timestep. This smoothing need only take a couple of meshpoints.

Acknowledgements

It is a pleasure to acknowledge useful conversations with Jonathan Sherratt concerning this work. EAG is grateful for the financial support of a Wellcome Trust Biomathematics Postdoctoral Training Research fellowship. Part of this work has been supported by the London Mathematical Society, under scheme 3.

REFERENCES

BARRANDON, Y. & GREEN, H. 1987 Cell migration is essential for sustained growth of keratinocyte colonies: The roles of transforming growth factor-α and epidermal growth factor. *Cell* **50**, 1131–1137.

BEEBE, D. & MASTERS, B. 1996 Cell lineage and the differentiation of corneal epithelial cells. *Investig. Ophthal. Visual Sci.* **37**, 1815–1825.

BERG, O. & VON HIPPEL, H. 1985 Diffusion controlled macromolecular interactions. *Ann. Rev. Biophys. Chem.* **14**, 131–160.

BORGENS, R., ROBINSON, K., VANABLE, J. JR., & MCGINNIS, M. 1989 *Electric Fields in Vertebrate Repair*. New York : A. R. Liss.

BUCK, R. C. 1985 Measurement of centripetal migration of normal corneal epithelial cells in the mouse. *Investig. Ophthal. Visual Sci.* **26**, 1296–1299.

CHIANG, M., ROBINSON, K.& VANABLE, J. 1992 Electric fields in the vicinity of epithelial wounds in the isolated bovine eye. *Exp. Eye Res.* **54**, 999–1003.

CHAN, K. Y., PATTON, D., & COSGROVE, Y. 1989 Time lapse videomicroscopic study of in vitro wound closure of rabbit corneal cells. *Investig. Ophthal. Visual Sci.* **30**, 2488–2498.

CHAN, K. Y., LINDQUAIST, T., EDENFIELD, M., NICHOLSON, M., & BANKS, A. 1991 Pharmacokinetic study of recombinant human epidermal growth factor in the anterior eye. *Investig. Ophthal. Visual Sci.* **32**, 3209–3215.

COOPER, M. 1984 Gap junctions increase the sensitivity of tissue cells to exogenous electric fields *J. Theor. Biol.* **111**, 123–133.

CRANK, J. 1987 *Free and Moving Boundary Problems*. Oxford: Clarendon Press.

CROSSON, C. E., KLYCE, S. D., & BEUERMAN, R. W. 1986 Epithelial wound closure in rabbit cornea. *Invest. Ophthalmol. Visual Sci.* **27**, 464–473.

DALE, P. D. 1995 Time Heals All Wounds? Mathematical Models of Epithelial and Dermal Wound Healing, D. Phil thesis. University of Oxford.

DALE, P. D., MAINI, P. K., & SHERRATT, J. A. 1994a Mathematical modelling of corneal epithelial wound healing. *Mathe. Biosci.* **124**, 127–147.

DALE, P. D., SHERRATT, J. A., & MAINI, P. K. 1994b On the speed of corneal epithelial wound healing. *Appl. Math. Lett.* **7**, 11–14.

DANJO, Y. & GIPSON, I. 1998 Actin 'purse strings' filaments are anchored by E-cadherin mediated adherins junctions at the leading edge of the epithelial wound, providing coordinated cell movement. *J. Cell Sci.* **111**, 3323–3332.

DICKINSON, R. B. & TRANQUILLO, R. T. 1995 Transport equations and biased cell migration based on single cell properties. *SIAM J. Appl. Math.* **55**, 1419–1454.

DUA, H., GOMES, J., & SINGH, A. 1994 Corneal epithelial wound healing. *Brit. J. Ophthal.* **78**, 401–408.

DUNN, G. A. & IRELAND, G. W. 1984 New evidence that growth in 3T3 cell cultures is a diffusion limited process. *Nature* **312**, 63–65.

ELLIOT, C. & OCKENDON, J. 1982 *Weak and Variational Methods for Moving Boundary Problems.* Research Notes in Mathematics, number 59, Boston, PA: Pitman.

FORRESTER, J. V., DICK, A., MCMENAMIN, P., & LEE, W. 1996 *The Eye.* London: W. Saunders.

FRIEDMAN, A. 1964 *Partial Differential Equations of Parabolic Type.* NJ: Prentice Hall.

GAFFNEY, E. A. 1999 Work in progress.

GAFFNEY, E. A., MAINI, P. K., & SHERRATT, J. A. 1997 Wound healing in the corneal epithelium: biological mechanisms and mathematical models. *J. Theor. Med.* **1**, 13–23.

GAFFNEY, E. A., MAINI, P. K., SHERRATT, J. A., & TUFT, S. 1999 A comparison of experimental data with a modelling framework for corneal epithelial wound healing. *J. Theor. Biol.* **197**, 15–40.

KLYCE, S. D. & BEUERMAN, R. 1988 Structure and function of the cornea. In: *The Cornea.* (H. Kaufman, B. Barron, M. Macdonald, & S. Waltman, eds.). New York: Churchill Livingstone.

MASTERS, B. 1995 Scanning slit confocal microscopy of the in-vivo cornea. *Optical Engin.* **34**, 684–692.

MCCAIG, C. D. & ZHAO, M. 1997 Physiological electrical fields modify cell behaviour. *BioEssays* **19**, 819–826.

OHASHI, Y., MOROKURA, M., KINOSHITA, Y., MANO, T., WATANABE, H., KINOSHITA, S., MANABE, R., OSHIDEN, K., & YANAIHARA, C. 1989 Presence of epidermal growth factor in human tears. *Investig. Ophthal. Visual Sci.* **30**, 1879–1882.

STA IGLESIA, D. D. & VANABLE, J. W. 1998 Endogenous lateral electric fields around bovine corneal lesions are necessary for and can enhance normal rates of wound healing. *Wound Repair Regen.* **6**, 531.

TSAI, L., MASTERS, B. & BEEBE, D. 1997 Coordination of mitosis and differentiation in the corneal epithelium. Meeting Abstracts. *Investig. Ophthal. Visual Sci.* **38**, 2281.

TSENG, S. 1989 Concept and application of limbal stem cells. *Eye* **3**, 141–157.

ZHAO, M., AGIUS-FERNANDEZ, A., FORRESTER, J. V., & MCCAIG, C. D. 1996a Orientation and directed migration of cultured corneal epithelial cells in small electric fields are serum dependent. *J. Cell Sci.* **109**, 1405–1414.

ZHAO, M., AGIUS-FERNANDEZ, A., FORRESTER, J. V., & MCCAIG, C. D. 1996b Directed migration of corneal epithelial sheets in physiological electric fields. *Investig. Ophthal. Visual Sci.* **37**, 2458–2558.

ZHAO, M., AGIUS-FERNANDEZ, A., FORRESTER, J. V., ARAKI-SASAKI, K., & MCCAIG, C. D. 1997 Bovine and human primary corneal epithelial cells and a transformed human cell line migrate directionally in an applied electric field. *Curr. Eye Res.* **16**, 973–984.

ZHAO, M., DICK, A., FORRESTER, J. V., & MCCAIG, C. D. 1999a Electric field directed cell motility involves up-regulated expression and asymmetric redistribution of epidermal growth factor receptors and is enhanced by fibronectin and laminin. *Mol. Biol. Cell* **19**, 1259–1276.

ZHAO, M., DICK, A., FORRESTER, J. V., & MCCAIG, C. D. 1999b A small physiological electric field orients cell division. *Proc. Natl. Acad. Sci. USA* **96**, 4942–4946.